

Light Pulse Slowing Down up to 0.025 cm/s by Photorefractive Two-Wave Coupling

E. Podivilov and B. Sturman

Institute of Automation and Electrometry, 630090 Novosibirsk, Russia

A. Shumelyuk and S. Odoulov

Institute of Physics, National Academy of Sciences, 252650 Kiev, Ukraine

(Received 24 April 2003; published 22 August 2003)

It is shown experimentally and theoretically that photorefractive wave coupling can be used for dramatic (≈ 0.025 cm/s) deceleration of light pulses whose width is larger than (or comparable with) the nonlinear response time. This classical nonlinear scheme exhibits similarities with the technique based on the quantum effect of electromagnetically induced transparency. The main distinctive feature of our scheme is amplification of the delayed output pulse. Advantages of the novel technique and its prospects for manipulation with light photons are discussed.

DOI: 10.1103/PhysRevLett.91.083902

PACS numbers: 42.65.Hw, 42.50.Gy, 78.20.Bh

Strong deceleration (down to the meter/second range), trapping, and coherent storage of light in atomic vapor have triggered in recent years a burst of research interest; see, e.g., [1–3], and references therein. This interest is greatly due to the promises for quantum information processing but also due to exciting physics of the mentioned new phenomena which are associated with the effect of electromagnetically induced transparency (EIT) [4]. Similar slow-light, trapping, and storage technique was proposed later for resonant solids [5].

Typically, a Λ scheme of atomic levels coupled by strong (pump) and weak (signal) resonant optical fields is in use to manipulate with photons in gases. The underlying quantum effect of EIT and creation of the so-called dark state [6] is here due to the joint action of the optical fields which produce a coherence between the lowest atomic levels [4]. The rise time T of this atomic coherence is inversely proportional to the pump intensity (to the square of the relevant Rabi frequency divided by the transverse relaxation constant) and the decrease of the initial absorption coefficient α is proportional to the degree of induced coherence. In the dark, the coherence decays with a very long time T_d [4,7].

The incident pulse signal is absorbed initially on the length $\approx \alpha^{-1}$ (which is much shorter than the cell thickness) and transformed into atomic coherence during the time $\approx T$. The corresponding layer becomes partially transparent. The pump transforms again the coherence into the signal wave. As a result, we have a coupled state of light pulse and atomic coherence (polariton) that propagates with the velocity $v_g \approx 2/\alpha T$ [3,8]. This velocity is proportional to the pump intensity and incomparably small against the light speed.

The effects of trapping, storage, and release of light pulses are most important under a strong difference between the rise time under illumination and the decay time of the atomic coherence in the dark, $T_d \gg T$. If the pump is switched off at a moment when the slowed down pulse is inside the medium, this pulse cannot leave the sample

and the excitation becomes recorded for a long time $\approx T_d$ in the form of quantum coherence. The stored coherence can be transformed into an outgoing pulse by switching the pump on upon demand.

The purpose of this Letter is to show experimentally and theoretically that the effects of dramatic slowing down, trapping, and storage of light pulses can be accomplished using an entirely new physical basis, namely, the photorefractive (PR) wave coupling [9]. In many respects, the proposed classical technique is similar to that based on the quantum nonlinear effect of EIT. But there are also important differences relevant to the apparent manifestations and experimental conditions. In particular, much lower pulse velocities can be obtained easily with the novel operation principle. To the best of our knowledge, the major aspects of the proposed technique were never considered within the PR domain.

Let two coherent waves of the same wavelength, a strong permanent pump and a weak signal pulse, be incident onto a PR sample, see Fig. 1. The light intensity is modulated at the spatial frequency \mathbf{K} (the grating vector) equal to the light wave-vector difference. Owing to spatial migration of photo-excited electrons (holes) a space-charge grating is built up. The rise time of the space-charge field τ is inversely proportional to the

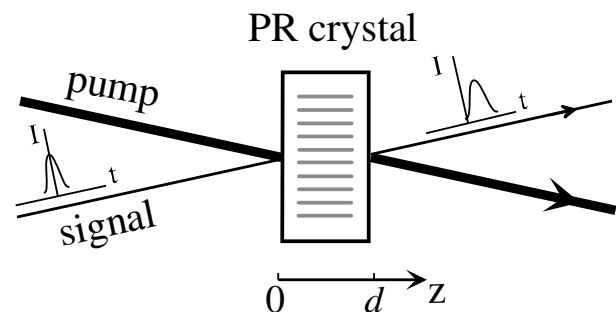


FIG. 1. A schematic of a pulse amplification experiment; the parallel lines inside the crystal depict the grating fringes.

pump intensity, whereas the dark decay time τ_d can be extremely long. Because of the linear electro-optic effect, the space-charge field produces a replica of refractive index; the pump and signal waves are coupled therefore via Bragg diffraction from the index grating.

Whereas the EIT nonlinearity results in a decrease of the light absorption coefficient, the function of the PR nonlinearity is to amplify the signal (absorption effects are typically small here). This makes the main difference between the above cases.

Consider qualitatively what happens with the pulse signal during its passage through the sample in the presence of the pump. The leading pulse edge travels almost freely because the index grating is very weak yet. The next portions of the pulse experience progressing spatial amplification because of increasing grating amplitude and, consequently, increasing diffraction from the pump beam. Moreover, buildup of the grating persists for a while after passing the signal maximum because of feeding of the signal wave via diffraction. As a result, the output pulse maximum is essentially delayed as compared to that of the input signal. The thicker the sample, the longer is the delay time.

The character of nonlinear pulse propagation depends on the type of charge transport. If diffusion of photo-excited carriers is the main transport mechanism, the index grating is $\pi/2$ shifted against the light interference pattern (the gradient nonlinear response). In this case, the energy can be permanently transferred to the signal. The main characteristic of the energy transfer is the rate of spatial amplification in steady state, Γ [9]; typically it does not depend on the light intensity and can be estimated as $\Gamma \approx (10-50) \text{ cm}^{-1}$ [9,10].

Most of our experiments are performed with a $\text{BaTiO}_3 : \text{Co}$ crystal. The input pulse shape was PC controlled via an electro-optic modulator; typically it was Gaussian. The main experimental parameters were as follows: The thickness $d = 2 \text{ mm}$, the wavelength $\lambda = 633 \text{ nm}$, the absorption coefficient $\alpha \approx 1 \text{ cm}^{-1}$, the input pump intensity $I_p \approx 3 \text{ W/cm}^2$, the input intensity ratio at the pulse maximum $I_p/I_s^{\text{max}} \approx 10^6$, the grating period $2\pi/K \approx 2.6 \mu\text{m}$, and the rise time $\tau \approx 3.5 \text{ s}$. No electric fields were applied, hence the charge separation is due to the diffusion transport. The light beams were extraordinarily polarized and the coupling strength Γd was estimated as ≈ 8 from auxiliary steady-state two-wave coupling experiments; this corresponds to $\Gamma \approx 40 \text{ cm}^{-1}$. Additionally, we used $\text{Sn}_2\text{P}_2\text{S}_6$ crystals showing a strong gradient response [11]. The rise time τ of this material is much shorter than that of BaTiO_3 .

Figure 2(a) shows representative experimental data for our BaTiO_3 sample and the input half-width of the pulse (at the half-intensity level) $w_0 \approx 0.76 \text{ s}$. One sees that the output pulse is substantially delayed and also broadened. The delay time of the pulse maximum is $\Delta t \approx 8 \text{ s}$. The effective velocity of the pulse maximum, $v_g = d/\Delta t$, can be estimated as $\approx 0.025 \text{ cm/s}$. Furthermore, it has been

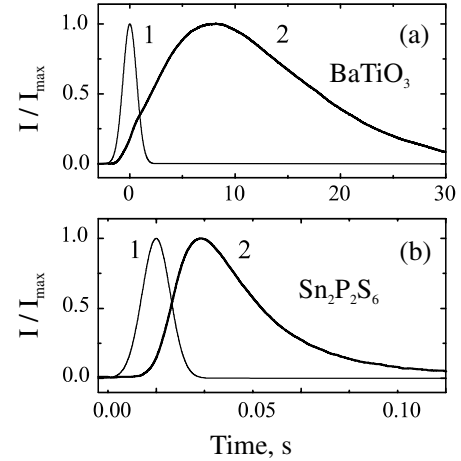


FIG. 2. Experimental time dependences of the normalized input and output intensities of the signal (curves 1 and 2, respectively) for BaTiO_3 (a) and $\text{Sn}_2\text{P}_2\text{S}_6$ (b) crystals.

checked that $(\Delta t)^{-1}$ is proportional to the pump intensity I_p within the range $(0.1-10) \text{ W/cm}^2$. Hence lower and higher pulse velocities are easily available. Similar results have been obtained with $\text{Sn}_2\text{P}_2\text{S}_6$ crystals, see Fig. 2(b), they correspond to $v_g \approx 40 \text{ cm/s}$.

Next, we present our results on modeling of the pulse propagation. Let P and S be the amplitudes of the pump and signal waves, respectively. Their dependence on the propagation coordinate z is caused by mutual Bragg diffraction from the refractive index grating and governed by the coupled wave equations [9]:

$$\left(\frac{\partial}{\partial z} + \frac{\alpha}{2}\right)S = \frac{\Gamma}{2} e P, \quad (1)$$

$$\left(\frac{\partial}{\partial z} + \frac{\alpha}{2}\right)P = -\frac{\Gamma}{2} e^* S, \quad (2)$$

where e is the normalized amplitude of the space-charge field. The total intensity, $I = |S|^2 + |P|^2$, decreases as $\exp(-\alpha z)$ during propagation. The time derivatives of S and P are omitted in Eqs. (1) and (2) because light follows adiabatically slow index changes; these derivatives are also of no importance under the conditions of slow-light experiments in gases [2,3].

The material equation for e , which supplements the set (1) and (2), reads as follows for the gradient PR response [9]:

$$\left(\tau \frac{\partial}{\partial t} + 1\right)e = \frac{SP^*}{|S|^2 + |P|^2} \quad (3)$$

with the response (rise) time $\tau \propto I^{-1}$. This time can often be identified as the dielectric relaxation time under light. The absolute value of the right-hand side is the half-contrast of the light intensity pattern.

Since $|S| \ll |P|$, we can use the undepleted pump approximation. Differential equations (1) and (3) form then a closed linear set for S and e . In steady state we would have from here $dS/dz = (1/2)(\Gamma - \alpha)S$. Usually, $\Gamma \gg \alpha$

in PR experiments and absorption effects are of no importance. Furthermore, we have found out that the set (1) and (3) is similar to the EIT equations. To make it catching the essence of the EIT pulse propagation, it is sufficient to set $\Gamma = \alpha$, $\tau = T$, and treat e as the atomic coherence degree; see, e.g., [12].

To solve the PR pulse propagation problem, we use the Fourier transform $S(z, t) \rightarrow S_\omega(z)$. With light absorption neglected, we have at the output, $S_\omega(d) = S_\omega(0) \times \exp[(\Gamma d/2)(1 - i\omega\tau)^{-1}]$, where $S_\omega(0)$ is the Fourier transform of the input amplitude $S(0, t)$. Generally, each input Fourier component gives a delayed output harmonic signal [13]. By making the inverse Fourier transform, one can find numerically the output intensity $|S(d, t)|^2$ for any particular shape of the input pulse. In accordance with experiment, we restrict ourselves to a Gaussian input beam, $S(0, t) = S_0 \exp(-t^2/t_0^2)$ with S_0 and t_0 being the input amplitude and width parameter (the input half-width $w_0 \approx 0.6t_0$). Then we have:

$$\frac{S(d, t)}{S_0} = \frac{t_0}{\sqrt{\pi}\tau} \int_0^\infty \exp\left(\frac{\Gamma d/2}{1+x^2} - \frac{x^2 t_0^2}{4\tau^2}\right) \times \cos\left[x\left(\frac{t}{\tau} - \frac{\Gamma d/2}{1+x^2}\right)\right] dx. \quad (4)$$

The right-hand side is a function of the normalized time t/τ ; it includes two dimensionless parameters, the ratio t_0/τ and the coupling strength Γd . Note the correspondence between the PR and EIT cases: If $|S(t/\tau; \Gamma d, t_0/\tau)/S_0|^2$ describes the normalized output signal on the basis of Eq. (4), then the function $\exp(-\alpha d) |S(t/T; \alpha d, t_0/T)/S_0|^2$ describes it as applied to the EIT case. In other words, the PR case is distinguished by the presence of an additional amplification factor $\exp(\Gamma d)$. The shape characteristics of the PR and EIT techniques are the same.

Figure 3 shows the output pulse shape for $t_0/\tau = 1$ and three values of the coupling strength; the trailing edge is to the right of the maximum. For $\Gamma d = 0$ we have free pulse propagation; the output profile is the same here as the input one. With the spatial amplification present, the output signal is remarkably delayed against the input one; the larger Γd , the longer is the delay time Δt and bigger the pulse amplification factor. Furthermore, pulse broadening is clearly seen in Fig. 3. The found features agree well with our experimental data.

For $\Gamma d \gg 1$, the delay time grows rather weakly with increasing t_0/τ and can be estimated as $\Delta t/\tau \approx \Gamma d/2$. Accordingly, the pulse velocity is $v_g = d/\Delta t \approx 2/\Gamma\tau$. The output pulse half-width w_d obeys the relation $w_d \approx (w_0^2 + \tau^2 \Gamma d \ln 2)^{1/2}$. For $w_0/\tau \geq (\Gamma d)^{1/2}$ the broadening effect is relatively weak, $w_d \approx w_0 \approx 0.6t_0$. If, additionally, $\Gamma d \geq 2t_0/\tau$, we have $\Delta t \geq w_0$, i.e., the output pulse is strongly delayed without noticeably changing its shape. This important regime occurs for sufficiently large values of the coupling strength, $\Gamma d > (10-12)$. An EIT equivalent

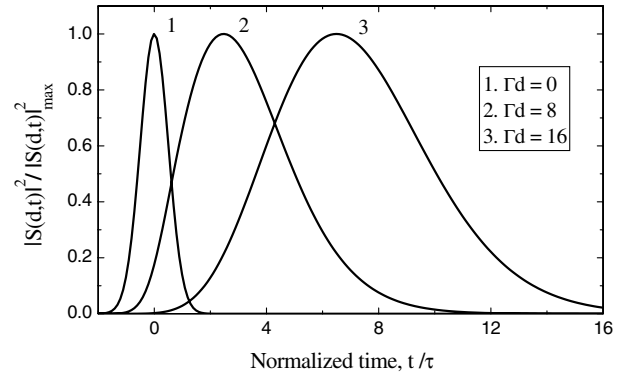


FIG. 3. The output signal shape for $t_0/\tau = 1$ and $\Gamma d = 0, 8$, and 16 ; the corresponding peak amplification factors are $1, \approx 2 \times 10^2$, and 3×10^5 .

of this case (with no spatial amplification and $\alpha d \approx 30$) has been realized in [1–3].

Figure 4 shows our experimental data on $\Delta t(t_0)$ and $w_d(t_0)$ for $\Gamma d \approx 8$ and the corresponding calculated curves. Agreement between theory and experiment (with no fit) is very good. In the intermediate region $t_0/\tau \sim 3$ we have a situation when $\Delta t \geq w_d \approx w_0$; this corresponds to a considerable delay of the pulse with only minor changing of its shape. The use of crystals with higher coupling strengths will allow one to get rid of the broadening effect.

In the limit $t_0 \ll \tau$ our theory predicts new qualitative features; see Fig. 5. For $t_0/\tau = 0.02$, the output pulse consists of a sharp nonshifted peak and a weak long tail possessing a maximum. With increasing t_0/τ , the tail is growing and the narrow peak is getting less and less pronounced. For $t_0/\tau = 0.2$ the nonshifted peak has fully disappeared and what we see at the output is a single delayed pulse which is strong and wide. The predicted peculiarities have been detected in our experiment; several left filled squares in Fig. 4 correspond to the

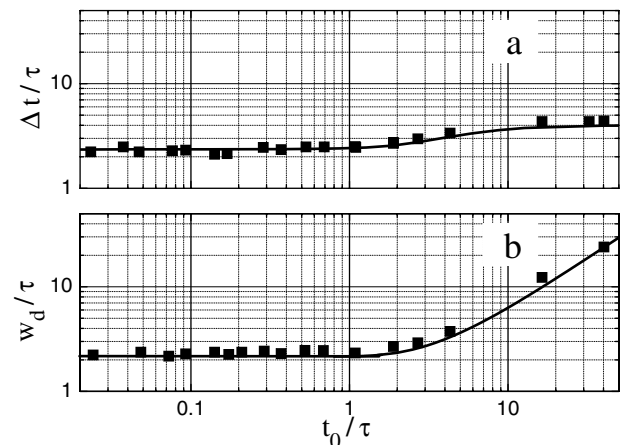


FIG. 4. The ratios $\Delta t/\tau$ (a) and w_d/τ (b) versus t_0/τ ; the squares are experimental data for BaTiO_3 and the theoretical lines are plotted for $\Gamma d = 8$.

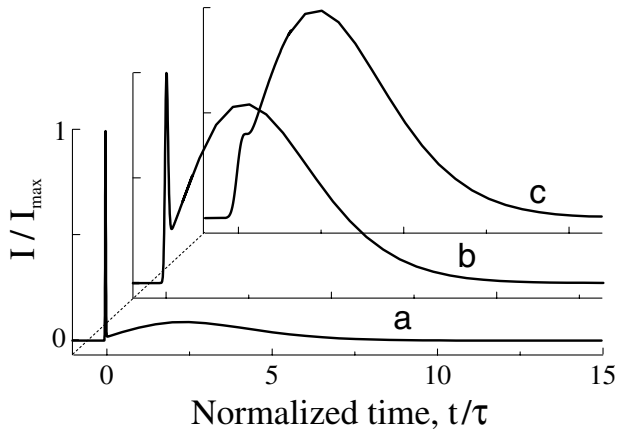


FIG. 5. The calculated normalized output intensity for $\Gamma d = 8$, and $t_0/\tau = 0.02$ [curve (a)], 0.08 (b), and 0.25 (c).

two-maxima region. In the EIT case, similar features can be expected for moderate values of αd .

We have reported on the main features of pulse propagation in a transmission geometry for the gradient response. PR nonlinearity offers, however, a much wider range of possibilities for slow-light experiments. These include the case of drift charge transport, when the phase shift between the light and index gratings is close to 0 or π [9], the case of resonant response relevant to excitation of low-frequency eigenmodes in fast PR materials [14], the use of reflection geometries when the light waves are incident onto the opposite crystal faces and the grating period is very small. Periodically poled materials offer additional advantages for pulse experiments because they combine an efficient buildup of index gratings with the absence of large-scale distortions of light beams [15].

The effects of pulse trapping, storage, and release, investigated widely in relation with the EIT phenomenon, are naturally inherent in the PR technique. The first of them is caused by an instantaneous disappearance of the diffracted signal and freezing for a long time of the recorded space-charge pattern upon switching off the pump. The PR effects of storage and release are due to readout of the frozen grating upon demand and its erasure by a strong readout beam. Specific features of the mentioned effects can, indeed, be different in PR and EIT domains.

Among the advantages of the PR technique is its broad spectral range (associated often with trap-band absorption shoulder), a wide acceptable temperature range (including room temperature), and the presence of many degrees of freedom for optimization and control of nonlinear optic characteristics. These include the spatial frequency, applied electric field, light polarization, and crystal cut.

At first sight, a serious drawback of the PR schemes is too long a response time τ ; it is about 6 orders of magnitude larger for our low-intensity experiments than the rise time $T \sim 10^{-6}$ s typical of EIT experiments with gases.

However, transition from the low-intensity (long-pulse) to high-intensity (short-pulse) experiments brings the response time $\tau \propto I_p^{-1}$ into the mks region [16,17] and makes the speed parameters competitive with those of the EIT schemes.

In summary, we have studied experimentally and theoretically light pulse propagation in PR media with the gradient nonlinear response. It is shown that the output pulse is characterized by a considerable time delay with respect to the input signal when the input pulse width w_0 is larger than (or comparable with) the characteristic rise time τ . This delay time grows almost linearly with increasing coupling strength and raises slowly with increasing w_0 . The pulse velocity is extremely small ($v_g \lesssim 0.025$ cm/s) as compared to the light speed; it is controlled by the pump intensity. There are clear similarities and differences between the EIT and PR techniques for manipulation with light pulses. The most important distinctive features of the PR scheme is amplification of the output pulse. Advantages of the PR technique and the prospects for further studies are discussed. The found effects can be useful for optical delay lines and also for material characterization.

We are grateful to Professor K. Buse for discussion and to Dr. A. Grabar and Dr. D. Rytz for $\text{Sn}_2\text{P}_2\text{S}_6$ and BaTiO_3 crystals.

-
- [1] L.V. Hau, S.E. Harris, Z. Dutton, and C. Behroozi, *Nature (London)* **397**, 594 (1999).
 - [2] C. Liu, Z. Dutton, C. Behroozi, and L. V. Hau, *Nature (London)* **409**, 490 (2001).
 - [3] D. F. Phillips, A. Fleischhauer, A. Mair, R. L. Walsworth, and M. D. Lukin, *Phys. Rev. Lett.* **86**, 783 (2001).
 - [4] S. E. Harris, *Phys. Today* **50**, No. 7, 36 (1997).
 - [5] N. C. Nielsen *et al.*, *Phys. Rev. B* **64**, 245202 (2001); M. S. Bigelow, N. N. Lepeshkin, and R.W. Boyd, *Phys. Rev. Lett.* **90**, 113903 (2003).
 - [6] E. Arimondo, *Prog. Opt.* **35**, 257 (1996).
 - [7] S. E. Harris and Y. Yamamoto, *Phys. Rev. Lett.* **81**, 3611 (1998).
 - [8] S. E. Harris and L.V. Hau, *Phys. Rev. Lett.* **82**, 4611 (1999).
 - [9] L. Solymar, D.J. Webb, and A. Grunnet-Jepsen, *The Physics and Applications of Photorefractive Materials* (Clarendon Press, Oxford, 1996).
 - [10] K. Buse, *Appl. Phys. B* **64**, 391 (1997).
 - [11] S. G. Odoulov *et al.*, *J. Opt. Soc. Am. B* **13**, 2352 (1996).
 - [12] M. Fleischhauer and M. D. Lukin, *Phys. Rev. Lett.* **84**, 5094 (2000); *Phys. Rev. A* **65**, 022314 (2002).
 - [13] D. Stateman, J. C. Lombardi, W. M. Shensky, and G. C. Gilbreath, *Opt. Commun.* **155**, 223 (1998).
 - [14] T. E. McClelland, D. J. Webb, B. I. Sturman, and K. H. Ringhofer, *Phys. Rev. Lett.* **73**, 3082 (1994).
 - [15] S. Odoulov *et al.*, *Phys. Rev. Lett.* **84**, 3294 (2000).
 - [16] A. L. Smirl *et al.*, *J. Opt. Soc. Am. B* **6**, 606 (1989).
 - [17] G. Pauliat and G. Roosen, *J. Opt. Soc. Am. B* **7**, 2259 (1990).